



Preconceptional paternal glycidamide exposure affects embryonic gene expression: Single embryo gene expression study following *in vitro* fertilization

Asgeir Brevik^{a,*}, Vendula Rusnakova^b, Nur Duale^a, Hege Holte Slagsvold^a, Ann-Karin Olsen^a, Ritsa Storeng^c, Mikael Kubista^d, Gunnar Brunborg^a, Birgitte Lindeman^a

^a Norwegian Institute of Public Health, Division of Environmental Medicine, Department of Chemical Toxicology, P.O. Box 4404, Nydalen, N-0403 Oslo, Norway

^b Dept. of Gene Expression, Institute of Biotechnology AS CR, v.v.i., Videnska 1083, Prague 4, 142 20, Czech Republic

^c Oslo University Hospital - Rikshospitalet, 0027 Oslo, Norway

^d Tataa Biocenter, Odinsgatan 28, 411 03 Göteborg, Sweden

ARTICLE INFO

Article history:

Received 2 March 2011

Received in revised form 10 August 2011

Accepted 17 September 2011

Available online 29 September 2011

Keywords:

Single-cell gene expression

Glycidamide

Acrylamide

Mouse embryo

ABSTRACT

Recognition of early determinants of disease onset has sparked an interest in paternally transmitted factors and their impact on the developing embryo. Acrylamide (AA), a widely distributed xenobiotic compound, is converted to its active metabolite glycidamide (GA) by the CYP2E1 enzyme. Based on its capacity to induce dominant lethal mutations, we hypothesized that paternal GA exposure would have a negative impact on embryonic genome activation, via GA-DNA and protamine adducts persisting in the fertilizing sperm. Using a combination of *in vitro* fertilization (IVF) techniques and RT-qPCR single embryo gene expression (SEGE), we studied the expression of key DNA repair genes and genes important for embryo development, at the 1-, 2-, 4- and 8-cell stage of the developing mouse embryo. Compared to controls paternal GA-exposure gave rise to an altered pattern of embryonic gene expression, with an initial reduced expression at early stages followed by increased expression at the 8-cell stage.

© 2011 Elsevier Inc. All rights reserved.

1. Introduction

A considerable part of infertility problems among couples is believed to be caused by male factors [1], and there is evidence of a decline in semen quality in many industrialized countries [2,3]. A parallel increase in testicular cancer observed over the last decades [4–6] raises concern over the impact of a modern lifestyle on the male reproductive system. Environmental factors are believed to be implicated in both the diminishing male reproductive health and the increased cancer incidence, but the part of the modern environment posing the greatest threat towards the male reproductive system has not been determined.

Germ line gene–environment interactions are currently being explored in an attempt to understand the dissonance between male reproductive health and the modern environment. Concern has been expressed on the possibility that paternal DNA damage is propagated across multiple generations. Post-meiotic male germ cells are sensitive to induction of heritable genomic damage particularly during the last few weeks of spermatogenesis [7,8]. All major DNA repair pathways seem to be less functional in late spermatids and sperm [9–12]. We have previously reported on excision repair activities in different testicular cell types [10,13–15] confirming

that DNA lesions are not repaired in late spermatids and sperm. High levels of DNA lesions are thus present in the sperm [15–17]. Embryonic development may be compromised when oocytes are fertilized with sperm containing higher than normal levels of DNA- and protamine-adducts.

Acrylamide (AA) is one of many chemicals that have been shown to induce DNA damage in the male germ line [18–20], dominant lethal mutations representing one critical consequence [20,21]. In addition to being an industrial chemical and a component of coffee and cigarette smoke, AA is formed by high temperature processing of glucose and, it is generally present at low levels in many carbohydrate rich fried foods like French fries, potato crisps, crisp bread, bread, and biscuits [22–24]. AA is oxidized to the reactive electrophilic epoxide glycidamide (GA) [25] by the CYP2E1 enzyme [26–28]. A large part of the damages attributed to AA exposure is believed to be caused by this reactive metabolite [26,28–30]. DNA and protamine alkylation have been suggested as mechanisms by which AA induces germ cell mutagenic effects [19,31,32], the most commonly reported DNA adducts being N7(2-carbamoyl-2-hydroxyethyl)-guanine (N7-GA-Gua) and to a lesser extent N3(2-carbamoyl-2-hydroxyethyl)-adenine (N3-GA-Ade) [26,33–35].

Global activation of the embryonic genome constitutes the most critical event at early stages of mammalian development. Maternal proteins and RNAs support development after fertilization, whereas a number of zygotic and embryonic genes are expressed

* Corresponding author. Tel.: +47 2107 6452.

E-mail address: asgeir.brevik@fhi.no (A. Brevik).

in a stage specific manner leading to embryonic genome activation [36]. The maternal to zygotic transition can be subdivided into two interrelated processes; first, a subset of the maternal mRNAs and proteins is eliminated; second, zygotic transcription is initiated [37]. The maternal to zygotic transition is a highly coordinated and extremely complex biochemical symphony and it has been estimated in the mouse that about 15,700 genes are expressed during preimplantation development [38]. Paternal exposure to the anti-cancer alkylating agent cyclophosphamide has been shown to alter the expression of DNA repair genes in the rat pre-implantation embryo [39,40]. A relevant question is whether less potent and more widely distributed environmental chemicals can affect the developing embryo via the same exposure route.

Based on our previous findings of very high levels of DNA lesions in sperm [15,16] and the ability of GA to form DNA and protamine adducts, we hypothesized that paternal preconceptional exposure to GA would have an impact on early embryonic transcription and on the activation of the embryonic genome. We studied the expression of key DNA repair genes and genes important to embryo development following paternal acute exposure to GA seven days prior to fertilization. To our knowledge this is the first time RT-qPCR single zygote/embryo gene expression techniques are used in studies on reproductive toxicity. We demonstrate that the early embryonic transcription of multiple genes is affected after paternal germ cells exposure to GA. The RT-qPCR single embryo gene expression technique has potential as a tool to study early developmental toxicity.

2. Methods

2.1. The exposure of male mice from which sperm was derived for IVF

Exposed males (strain B6D2F1 from Charles River Laboratories, 8–12 weeks of age) received one i.p. injection of GA (61 mg/kg body weight) dissolved in phosphate buffered saline eight days prior to the IVF experiment. Timing of the exposure to GA was based on pilot studies and knowledge about the most susceptible stage of spermatogenesis with respect to dominant lethal mutations. Similarly aged control males received an equivalent volume of phosphate buffered saline. At the day of the IVF experiment males were killed by cervical dislocation. Cauda were surgically removed and collected in an eppendorf tube containing M2 medium (500 μ l, Sigma). Using a pair of micro scissors a few incisions were made in the cauda and the sperm was allowed to disperse for 10 min in a small drop (250 μ l) HTF medium (EmbryoMax, Millipore) under liquid paraffin (MediCult) before transfer to the IVF dishes. Experiments are based on oocytes from 75 females and sperm from 10 males (5 exposed and 5 controls) altogether.

2.2. Super-ovulation and in vitro fertilization (IVF)

Females (strain B6D2F1 from Charles River Laboratories, 4–6 weeks of age) were injected i.p. with pregnant mare serum hormone gonadotropine (PMSG, Folligon from Intervet) (5 IU) three days prior to the IVF procedure. Two days later (that is, the day before the IVF) animals received an additional i.p. injection of human chorionic gonadotropine (HCG, Ovitrelle from Serono) (5 IU). Mice were killed by cervical dislocation and oviducts were collected in M2 medium (Sigma). Egg clutches (10–20 oocytes) embedded in cumulus cells were extracted from each oviduct. Oocytes were transferred to IVF-dishes and incubated in a droplet of HTF sperm containing medium under liquid paraffin for 4.5 h (37 °C). Oocytes from one side of the animal were combined with sperm from gydamide exposed animals and oocytes from the other side were combined with sperm from control animals. Hence, oocytes from all animals were present in both the control group and the exposed group. After 4.5 h the fertilized oocytes (zygotes) were washed 5 \times in KSOM medium (EmbryoMax Millipore) before they were transferred to a drop of KSOM (200 μ l) in a petri dish (35 mm) under liquid paraffin (MediCult). Samples from the 1-cell stage were collected immediately after fertilization. The rest of the zygotes were allowed to grow to harvest at the 2-cell, 4-cell or 8-cell stage. Upon harvest zygotes/embryos were collected in micro tubes filled with 5 μ l lysis medium (CelluLyser, TATAA) and then frozen at –70 °C.

2.3. Reverse transcriptase and cDNA synthesis

Samples were thawed before a total of 14.5 μ l mastermix and reverse transcriptase enzyme (Roche transcriptor first strand cDNA synthesis kit, Cat no. 04896866001) was added to all samples. The samples were then incubated in a thermal cycler unit (Eppendorf mastercycler) according to the following protocol:

10 min at 25 °C, 30 min at 50 °C, 5 min at 85 °C, and then held at 4 °C. After the RT reaction was completed samples were again frozen at –70 °C.

2.4. Preamplification of cDNA

Preamplification was used to increase the number of template molecules. This is a necessary step because the cDNA synthesis does not yield sufficient number of molecular copies of the template molecules which can be analyzed with confidence in parallel singleplex reactions. A high similarity between the gene expression measurements of preamplified and non-preamplified samples has been reported [41]. Preamplification PCR was run in 20 μ l volume containing 4 μ l of cDNA, 2 μ l of a mixture of all forward and reverse primers (500 nM each), 10 μ l of AmpliTaq Gold360 Master mix (Applied Biosystems) and water. PCR primers were designed using the online Universal Probe Library System from Roche. A CFX 96 cycler (Bio-Rad) was used for the preamplification with the cycling conditions: polymerase activation at 95 °C for 10 min, followed by 18 cycles (95 °C 15 s, 59 °C 1 min and 72 °C 1 min). The product of the preamplification reaction was diluted to 80 μ l and stored at –20 °C. The robustness of the preamplification was validated by comparing qPCR expression levels of Chek (highly expressed) and Mlh3 (typically low expression) with and without preamplification in tissues from liver, ovary and embryo. The relative expression of the two genes was similar when analyzing data with and without preamplification.

2.5. High throughput qPCR

The sample reaction mixture had a volume of 5 μ l and contained 1 μ l of preamplified cDNA, 0.5 μ l of SYBR Green Sample Loading reagent (Fluidigm), 2.77 μ l AmpliTaq Gold360 Master mix (Applied Biosystems), 0.165 μ l of Chromofy, diluted 1:25 (TATAA), 0.025 μ l of ROX (Invitrogen). The primer reaction mixture had a final volume of 5 μ l and contained 2.5 μ l Assay Loading Reagent (Fluidigm) and 2.5 μ l mixture of reverse and forward primers corresponding to a final concentration of 5 μ M. The chip was first primed with an oil solution in the NanoFlex™ 4-IFC Controller (Fluidigm) to fill control wells of the dynamic array. Bubbles were carefully removed from the 5 μ l reaction mixture and the mix was loaded into the sample wells, and 5 μ l of the primer reaction mixtures was loaded into the assay wells of the dynamic array. The dynamic array was then placed in the NanoFlex™ 4-IFC Controller for automatic loading and mixing. After 55 min the dynamic array was transferred to the BioMark qPCR platform (Fluidigm). The cycling program was 10 min at 95 °C for preactivation, followed by 30 cycles of denaturation at 95 °C for 15 s, annealing at 60 °C for 20 s, and elongation at 72 °C for 20 s. After completed qPCR cycling melting curves were collected between 60 and 95 °C with 0.5 °C increments.

2.6. qPCR basic data analysis

The BioMark qPCR platform is primarily designed for Taqman probes. Here we used next-generation Chromofy as an unspecific dye binding double stranded DNA with higher affinity and fluorescence compared to regular SYBR Green. Chromofy has excitation/emission spectra similar to FAM. Since there is no separate set up for Chromofy in the Biomark qPCR platform, we used FAM-MGB settings with slightly altered exposition temperature and a linear baseline correction derived from independent experiments (data not shown). ROX (emission at 645 nm) was always used for passive signal normalization.

2.7. Data preprocessing

Normalization of qPCR data is often done relative to the expression of reference genes, number of cells, weight of tissue (DNA/RNA spike) or total RNA concentration. Expression of mouse reference genes in temporal development of an embryo will not be constant and hence will likely introduce unwanted variability. As a consequence we chose to not use endogenous reference genes in the present study, in line with recommendations from Sindelka et al. [42]. By not using endogenous reference genes emphasis was put on careful and highly standardized technical handling.

To ensure that measurements at low levels were well within the linear area of detection, all C_q values above 26 were coded as missing values. In addition, embryos with gene expression pattern radically different from the overall group mean were classified as outliers. The excluded outliers most likely represented deteriorating embryos that were about to die. Filtering criteria for missing values was set to 70%, which is the minimum percentage of existing values, and all the patterns with less than 70% existing values were removed. All estimates are mean values based on 10–15 single zygotes/embryos.

The information contained in the biological replicates was used to replace missing values in the remaining biological replicates when available. If all biological replicates gave missing data, they were all assigned the highest measured C_q of that particular gene +1. Since the highest measured C_q of a truly positive sample can be assumed to be the limit of detection (LOD) for that particular gene, assigning $C_q(\text{LOD}) + 1$ to the off-scale samples corresponds to a concentration that is half of the LOD. Relative expression (RQ) among the sample was calculated as [41]:

$$RQ = 2^{C_{q\text{min}} - C_q}$$

Table 1
The genes included in the present analysis and their main function.

Symbol	Common name	Major function
Chek1 ^a	Checkpoint homolog (<i>Schizosaccharomyces pombe</i>)	P53 signaling
Mlh3	mutL homolog 3	DNA repair
Xpa ^b	Xeroderma pigmentosum, complementation group A	DNA repair
Ercc2	Excision repair cross-complementing rodent repair deficiency 2	DNA repair
Zbed3 ^a	Zinc finger, BED-type containing 3	DNA repair
Pms2 ^a	Mismatch repair endonuclease (postmeiotic segregation increased 2)	DNA repair
Prm2	Protamine 2	Sperm marker
Hdac1	Histone deacetylase 1	Epigenetic signaling
Ercc3	Excision repair cross-complementing rodent repair deficiency 3	DNA repair
Pcna ^a	Proliferating cell nuclear antigen	Embryo development
Spin1 ^b	Spindlin 1	Embryo development
Pms1 ^a	Postmeiotic segregation increased 1 (<i>Saccharomyces cerevisiae</i>)	DNA repair
Dnmt1 ^b	DNA (cytosine-5-)-methyltransferase 1	P53 signaling
Poib ^b	Polymerase (DNA directed), beta	DNA repair
Kdm4a ^b	Lysine (K)-specific demethylase 4A	Epigenetic signaling
Xrcc1	X-ray repair cross complementing protein	DNA repair
Ercc1	Excision repair cross-complementing rodent repair deficiency 1	DNA repair
Tp53 ^a	Tumor protein p53	P53 signaling
Nanog ^a	Nanog homeobox	Embryo development
Kdm4c ^a	Lysine (K)-specific demethylase 4C	Epigenetic signaling
Msh2	mutS homolog 2, colon cancer, nonpolyposis type 1 (<i>Escherichia coli</i>)	DNA repair
Ddb2	Damage-specific DNA binding protein 2	DNA repair
Mpg	N-methylpurine-DNA glycosylase	DNA repair
Pou5f1	POU class 5 homeobox 1	Embryo development
Cdh1	Adherin 1, type 1, E-cadherin (epithelial)	Embryo development
Ddb1	Damage-specific DNA binding protein 1	DNA repair
Fgfr2	Fibroblast growth factor receptor 2	Embryo development
Tdp1	Tyrosyl-DNA phosphodiesterase 1	DNA repair
Mre11a ^a	Meiotic recombination 11 homolog A (<i>S. cerevisiae</i>)	DNA repair
Tgfb1	Transforming growth factor, beta 1	Embryo development
Ogg1	8-Oxoguanine DNA glycosylase	DNA repair
Lig3	Ligase III, DNA, ATP-dependent	DNA repair
Dppa3	Developmental pluripotency associated 3	Embryo development
H2afz	H2A histone family, member Z	Embryo development
Mos	Oocyte maturation factor mos	Embryo development
Gtf2h3	General transcription factor IIH, polypeptide 3	DNA repair
Npm2	Nucleophosmin/nucleoplasmin 2	Sperm marker
Crabp1 ^b	Cellular retinoic acid binding protein 1	Embryo development
Gapdh ^b	Glyceraldehyde-3-phosphate dehydrogenase	Metabolism/control gene

^a Genes that responded to paternal GA exposure.

^b Genes that were mainly off-scale (excluded from the analysis).

For each gene ΔCq values were calculated by subtracting Cq from the lowest sample Cq , and then converting the difference to linear scale, as shown in the equation above. These relative quantities (RQ) indicate the level of expression, in each sample, of a particular gene relative to the sample in which the gene has the highest expression. Hence, the RQ of the sample with highest expression is set to one and all other samples for that gene have $RQ < 1$.

For further analysis with classic parametric tests, such as Student's t -test, linear regression and Anova, data must be normally distributed. Gene expression data are usually not normally distributed when expressed as relative quantities, but they will become normally distributed after logarithmic transformation to fold difference (FD). Traditionally log base 2 is used.

$$FD = \log_2(RQ)$$

Fold differences are equivalent to the corresponding delta Cq values for the purpose of statistical analysis. However fold differences provide useful control of the relative pivot point as defined by the RQ transformation step, the latter being preferred for visualization purposes.

2.8. Data scaling

Mean centering was performed to avoid highly expressed genes from being allowed to carry too much weight. The effect of the gene expression level was removed by subtracting the mean expression of every gene to the corresponding gene. For mean centered data a certain deviation from normal expression has the same weight independent of the expression level [41].

$$FD_{MC} = FD - \overline{FD}$$

Using the approach outlined above we compared differences in gene expression between developing mouse embryos originating from fertilization by spermatozoa from GA exposed fathers relative to control fathers right after fertilization, and at the 2-, 4- and 8-cell stages of embryo development.

2.9. Statistical analysis

Results are presented as the mean \pm SEM. Student's t tests were used to test for differences between embryos of exposed fathers relative to control embryos. Values were considered to be significantly different when $p < 0.05$.

3. Results

Zygotes and embryos from four pre-implantation stages (1-, 2-, 4- and 8-cell) fertilized either with control sperm or with sperm from GA treated mice, were used to study the effect of paternal exposure to GA on the expression of a panel of 39 genes involved in DNA damage response and embryo development. These genes were selected based on prior knowledge and literature mining. The 39 genes are listed in Table 1.

3.1. Sample extraction and fertilization

A total of 105 zygotes/embryos (43 derived from GA exposed sperm and 62 from control sperm) at 4 different developmental stages were used for the final analysis. The number of embryos analyzed from each stage after pre-processing is shown in Table 2.

Known to vary between different strains of mice, the 1st (1–2) and 2nd (2–4) cell cycles of the embryo take between 16–20 h and 18–22 h, respectively [43,44]. In the current experiment we timed our sample extraction according to 24 h cycles; 2-, 4- and 8-cell time points equals 24, 48 and 72 h,

Table 2
The number of embryos in each treatment group after RT-qPCR pre-processing.

Stage	Group	Median	Range
1 cell	Control	17	11–17
	Exposed	14	7–14
2 cell	Control	13	9–13
	Exposed	12	9–12
4 cell	Control	16	9–16
	Exposed	11.5	5–13
8 cell	Control	11	8–11
	Exposed	10	6–10
Total	Control	56	46–57
	Exposed	46	36–49

respectively. Stages can be readily identified up to the 8-cell stage and careful visual inspection served as additional quality criteria upon sampling. Overall, cell cycle length is subject to considerable variation, not only among different embryos, but also among blastomeres within the same embryo [45–47].

For the 1-cell fertilized samples, both exposed and controls were collected immediately after the IVF procedure. Isolation of successful fertilizations was based on the appearance of polar bodies on the oocyte cell surface of healthy looking oocytes, when these were visible. Crude correlations based on RT-qPCR results indicate a clear difference between fertilized and unfertilized oocytes in terms of gene expression (supplementary figure 1), and this may tentatively be taken as a sign of successful fertilization. Samples from the 2-, 4- and 8-cell stage were exclusively chosen from the pool of structurally healthy looking embryos representative of the relevant stage.

3.2. Pre-processing and results from single cell RT-qPCR

Only those genes that passed the quality assurance criteria described in Section 2 were included in the down-stream analysis. From a total of 39 genes, a filtered list consisting of a matrix of dimension 30 genes \times 43 GA exposed sperm derived embryos was used to search for transcripts showing fold differences (between embryos fertilized with sperm from GA-treated mice and those fertilized with control sperm from the same embryonal stage). The 43 GA exposed sperm derived embryos and the 62 control embryos were from four preimplantation stages (1-, 2-, 4- and 8-cell). Each stage consists of at least nine biological replicates. The fold difference in gene expression was derived by dividing each normalized relative quantity value by the average of stage-matched control values (RQ-value of treated embryo – RQ-value of average stage-matched control embryos). Gene expression levels are hence always relative to the control embryos at the same embryonal stage. The obtained gene expression ratios were used in the down-stream analysis.

An unsupervised hierarchical clustering analysis (average-linkage and Euclidean distance similarity measurement) was used to cluster genes and samples into groups based on their similarity, and the results were visualized in a dendrogram (Fig. 1). The dendrogram shows the similarity of the genes (rows), and similarity of the samples (columns) (Fig. 1). Although the row dendrogram and the column dendrogram are shown simultaneously on the heatmap, they are computed independent of each other. Fig. 1 shows the clustering analysis of gene expression alterations across embryo developmental stages. The clustering dendrogram of the 43 embryos from GA exposed sperm reveals two distinct branches: the first branch consists of embryos from 1- and 2-cell and some from the 4-cell stage, while all 8-cell stage and some 4-cell stage embryos were clustered close to each other in the second branch (Fig. 1). With a few exceptions, we observed an overall tendency

towards reduced expression at the 1- and 2-cell stage together with an increased gene expression at the 8-cell stage in embryos of GA exposed fathers compared to controls (Fig. 1).

Genes with similar temporal expression patterns over a range of embryo development stages might share common regulators. Co-regulated and functionally related genes are probably going to be expressed (up and down) simultaneously, and will hence appear as clusters. One way to detect co-regulated genes is to investigate whether genes with similar expression patterns belong to the same cluster. By inspection of the clustering dendrogram, we observe the 30 genes studied cluster in three branches (Fig. 1). Group I consists of seven genes: *Cdh1*, *Dppa3*, *H2afz*, *Kdm4c*, *Msh2*, *Pou5f1* and *Xrcc1*, Group II consists of 18 genes: *Chek1*, *Ddb1*, *Ddb2*, *Erc1*, *Erc2*, *Erc3*, *Hdac1*, *Lig3*, *Mlh3*, *Mos*, *Mpg*, *Mre11a*, *Pcna*, *Pms1*, *Pms2*, *Tdp1*, *Fgfr2* and *Trp53*, while Group III consists of five genes: *Gtf2h3*, *Nanog*, *Npm2*, *Ogg1* and *Zbed3*. We then used the MouseNet server (<http://www.functionalnet.org/mousenet/>) to investigate the connectivity or co-occurrence network of these 30 genes. The interactions between these genes are constructed by Cytoscape® software [48], and shown in Fig. 2.

In Fig. 3 relative gene expression for the genes that were expressed significantly different between control embryos and embryos of GA exposed fathers is shown. A general trend of an initial down-regulation at 1- and 2-cell stage, followed by an up-regulation at the 8-cell stage seems to be present.

A separate single experiment was performed to study potential differences in development between control embryos and embryos of GA exposed fathers. The results suggest that there was a slightly lower formation of 2-celled embryos following fertilization with sperm from GA exposed fathers compared to controls (80% and 92%, respectively). Several of the embryos of GA exposed fathers also seemed to have slightly delayed development into the blastocyst stage.

4. Discussion

We have previously shown that DNA lesions induced in late spermatids or sperm persist in the sperm [15–17]. The consequences of paternally transferred DNA lesions are however still unclear. With respect to GA exposure heritable genomic changes and dominant lethal effects are most evident after exposure to these later stages of spermatogenesis and spermiogenesis [49,50], and it is likely that these effects are associated with persistent DNA- and protamine-adducts present in the fertilizing sperm. In this work we have investigated whether paternal exposure to GA at the spermatozoa stage has implications for gene expression during early embryo development. We have selected embryos with normal appearance at each stage in order to study responses different from those involved in preimplantation embryo lethality, which occurs at higher exposure doses. The most apparent effects observed in embryos of GA exposed sperm were that gene expression at the 1- and 2-cell embryonic stages were down regulated relative to controls followed by an up-regulation at the 8-cell stage.

The formation of GA-induced DNA and protamine adducts represents, the most likely mechanism by which parental GA-exposure impacts gene expression in the ensuing embryo, although other cellular mechanisms may also come into play. Protamine adducts are thought to introduce stresses in the sperm chromatin structure that are converted into DNA strand breaks upon fertilization. Such DNA lesions are repaired in the zygote, but may cause an increase in chromosomal aberrations if unrepaired as shown in zygotes from acrylamide exposed male mice [51]. In contrast, the major GA induced DNA adduct (N7-(2-carbamoyl-2-hydroxyethyl)guanine; N7-GA-Gua) has a slow repair kinetic [33,34] and is likely not fully removed before the first cleavage

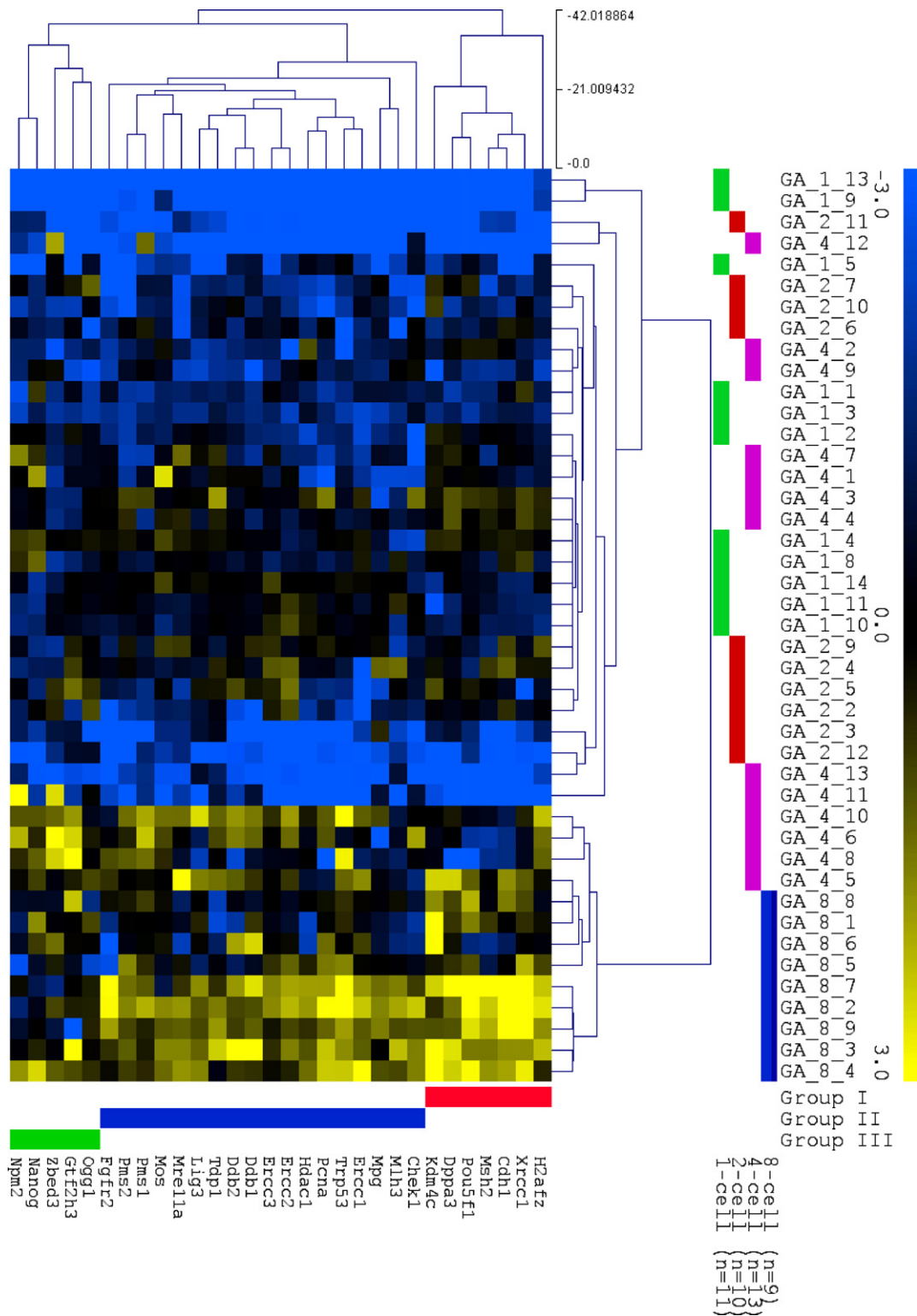


Fig. 1. The heatmap shows relative gene expression after normalization and mean-centering of the data. An unsupervised hierarchical clustering analysis based on similarities in gene expression is included in the heatmap. Row and column dendrograms are computed independently of each other. Yellow samples represent up-regulated gene expression whereas bright blue samples represent down-regulated gene expression compared to average (black). Horizontal color bars indicate cell stage, vertical color bars indicate clustering after hierarchical clustering analysis. (For interpretation of the references to color in the figure caption, the reader is referred to the web version of the article.)

division. It is possible that other effects, beyond direct protamine and DNA adduct formation, could have contributed to the characteristic pattern of gene expression observed in the present study. The fact that the major reprogramming in the mouse embryo does

not start until the 2-cell stage could indicate epigenetic effects as being responsible for the initial reduction in gene expression seen in embryos of GA exposed sperm compared to controls. There is convincing evidence that at least six components of the sperm

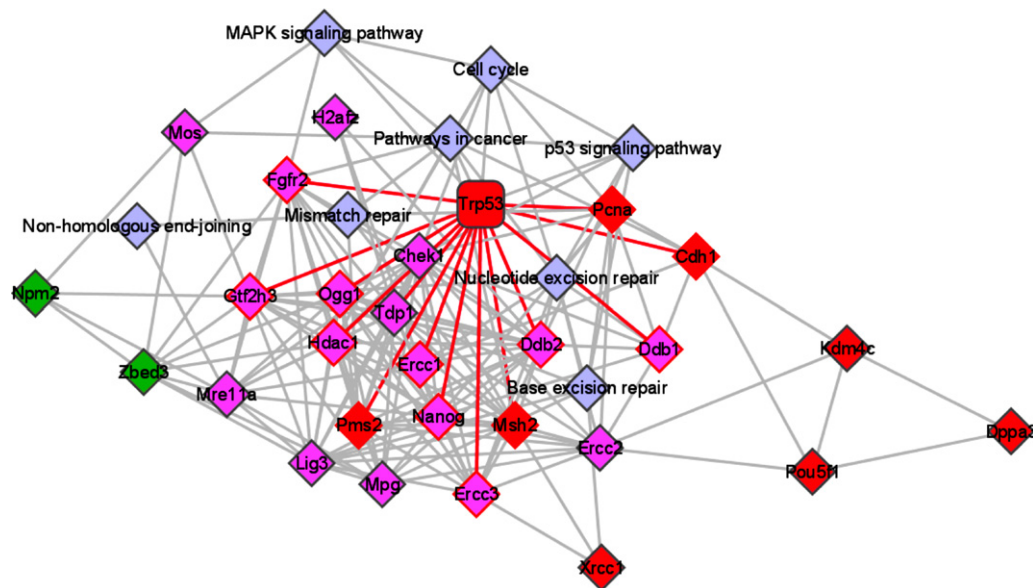


Fig. 2. A network analysis is shown indicating expression levels and connections at the 8 cell stage. Red symbols indicate genes that are up-regulated, whereas green symbols indicate genes that are down-regulated in embryos of exposed fathers relative to controls. Pathways are indicated by blue symbols. Red lines indicate connections to the p53 protein. (For interpretation of the references to color in the figure caption, the reader is referred to the web version of the article.)

nucleus are inherited from the paternal nucleus; DNA-methylation, sperm-specific histones, other chromatin-associated proteins (e.g. topoisomerase II), the perinuclear theca proteins, sperm-borne RNAs and the DNA-loop domain organization by the sperm nuclear matrix [52].

A separate IVF experiment was performed to test for potential differences in fertilization rates and developmental milestones among controls and embryos of GA exposed fathers. Based on these results, several embryos of GA exposed fathers seemed to have a delayed development into the blastocyst stage compared to controls. The suppressed transcription observed in GA exposed sperm derived embryos at the 1- and 2-cell stage could not simply be interpreted as an increased propensity of these cells to undergo apoptosis. It has been demonstrated by others that cell cycle checkpoints and apoptosis are largely absent in early stages of mouse embryo development [53–57].

The fact that paternal exposure can affect gene expression of the developing embryo justifies concern about potential human health effects manifested in the next generation. Trans-generational effects of DNA adducts have been reported previously. Smoking may serve as a classical example of xenobiotic exposure with potential transgenerational health effects. Sperm from smoking males typically exhibit higher levels of DNA fragmentation and base adduct formation [7]. Sperm from smoking males still retain their capacity to fertilize the oocyte, but it has been reported that the offspring of smoking males experience higher incidence of childhood cancer [8,58]. These studies exemplify the concept of paternal germ cell DNA damage creating undesired effects in the offspring.

Effects of paternal exposure manifested at the 2-cell stage of embryo development have been documented by other investigators. Marchetti et al. reported increased levels of chromosomal mosaicism in 2-cell mouse embryos after paternal

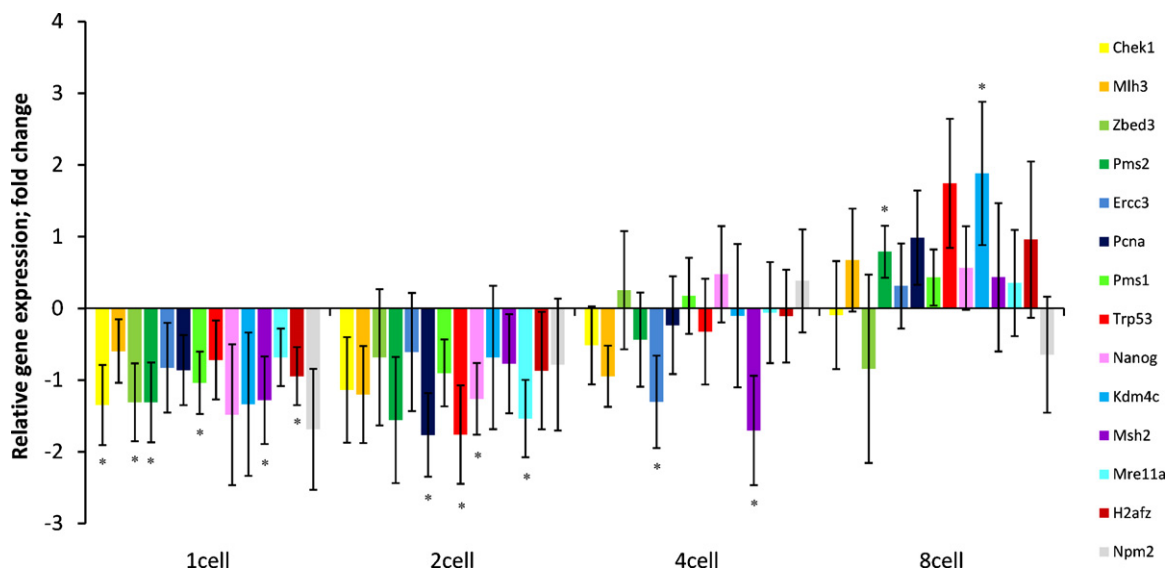


Fig. 3. Relative gene expression is shown for the genes that at some point during the 72 h study period responded significantly to paternal preconceptional exposure to GA. Results are mean values (\pm standard error).

exposure to acrylamide [59]. In another report cyclophosphamide, a widely used anti-cancer agent has been found to alter epigenetic histone H4 acetylation and methylation in preimplantation rat embryos at the 2-cell stage [60]. Paternal cyclophosphamide exposure has also been shown to induce DNA damage in the rat zygote [61] and to induce an altered expression of several DNA repair genes in cleavage stage embryos [39].

With respect to technical details in this experiment, the exposure level of GA is much higher than would be expected in a natural environment. Sperm protamine and DNA adducts are not repaired, and repeated acrylamide exposure leads to an accumulation of acrylamide induced chromatin adduction [32]. Using a single exposure enabled us to study the consequences of a defined exposure of the spermatozoa in a maturation stage strongly associated with induction of dominant lethality and heritable translocations. The dose chosen was lower than those used for studying dominant lethality [21,62,63], but slight to moderate increases in heritable translocations and chromosomal aberrations is reported at comparable levels in studies using acrylamide [51,64]. New studies are needed to examine potential gene expression perturbations in the developing embryo after chronic low-dose paternal exposure to relevant environmental exposures.

In contrast to the general down-regulation at the 1- and 2-cell stage, the transcriptional up-regulation observed in GA exposed sperm derived embryos at the 8-cell stage does not apply to all genes. The slightly more differentiated pattern at the latter stage could perhaps indicate that a more specific cellular response has been initiated in an attempt to deal with molecular damage inherited from GA exposed male germ-cells.

Among the DNA repair genes investigated Pms2 was significantly up-regulated at the 8-cell stage in the GA exposed sperm derived embryos compared to the controls. This gene, located on chromosome 7, codes for a DNA mismatch repair protein. It forms a heterodimer with MLH1 and this complex interacts with other complexes bound to mismatched bases. Mutations in these genes are associated with hereditary non-polyposis colorectal cancer (Lynch syndrome) [65]. Moreover, Pms2 is implicated in DNA damage signaling, a process which induces cell cycle arrest and can lead to apoptosis in case of major DNA damages. The up-regulation of this gene is consistent with the idea that the cell cycle may be arrested and with apoptosis being induced.

Embryos of GA exposed fathers were also found to have significantly increased expression of the histone demethylase Jmjd2C/Kdm4C at the 8-cell stage. In one study Jmjd2C/Kdm4C knockdown caused decreased proliferation of tumor cells, suggesting a contribution of Jmjd2C/Kdm4C to tumor growth [66]. Over-expression of Jmjd2C/Kdm4C has been found to enhance the expression of the Mdm2 oncogene [67].

We were not able to pinpoint clear-cut mechanistic reactions based on the horizontal branching of the dendrogram (Fig. 1). However, in a separate network analysis many of these genes were found to be p53 target genes (Fig. 2), and several of them even have p53 binding sites. The p53 association is interesting even though p53 signaling is not very well characterized at these early stages of development. In studies of preimplantation mouse embryos fertilized with sperm exposed to gamma irradiated paternal DNA damage did not severely reduce fertilization rates and implantation, but radiation reduced the number of fetuses [68–70]. Sperm irradiation resulted in a suppression of DNA synthesis in the zygote. The S-phase delay in the zygotes was p53-dependent and seemed to be dependent on p53 DNA-binding, but not on p53 transcriptional activity [68–70]. Although a more differentiated response of embryos of GA exposed sperm is witnessed at the 8-cell stage compared to the 1- and 2-cell stage, we believe that the increased expression in some of the genes at this stage is best interpreted

as being caused by an overall effect on the embryo rather than being clearly confined to particular pathways. A conservative evaluation of the genes that responded significantly is advisable. The overall tendency towards reduced gene expression at the 1-, and 2-cell stage followed by the increased expression at the 8-cell stage constitutes our most important observation. New dose-response studies should look at the consistency of the characteristic pattern of 1- and 2-cell down-regulation and 8-cell up-regulation across different doses. There is a need for more information on low-dose periconceptional toxicity, and gene expression analyses such as these may provide one tool for a much sought after quantitative evaluation of subtle gene or gene network perturbations that should be acknowledged in risk evaluations.

In summary early embryonic gene expression is affected by pre-conceptional paternal exposure to glycidamide. Persisting paternal GA DNA and protamine adducts or epigenetic changes are probable mechanisms to cause altered expression of genes related to embryonic stem cell pluripotency, DNA repair, and methylation dynamics in early mouse embryos. Single embryo gene expression represents a new technique with potential to advance our understanding of both reproductive toxicity and the extremely complex process of embryo development.

Conflict of interest

Stock Ownership: M. Kubista, TATAA Biocenter.

Acknowledgements

This work was supported by The Research Council of Norway, grant # 182048/V40, and The Grant Agency of Academy of Science Czech Republic (IAA500520809) and research goal AV0Z50520701 granted by Ministry of Youth, Education and Sports of the Czech republic.

Appendix A. Supplementary data

Supplementary data associated with this article can be found, in the online version, at doi:10.1016/j.reprotox.2011.09.005.

References

- [1] Hotaling JM, Walsh TJ. Male infertility: a risk factor for testicular cancer. *Nat Rev Urol* 2009;6(October (10)):550–6.
- [2] Auger J, Kunstmann JM, Czyglik F, Jouannet P. Decline in semen quality among fertile men in Paris during the past 20 years. *N Engl J Med* 1995;332(February (5)):281–5.
- [3] Carlsen E, Giwercman A, Keiding N, Skakkebaek NE. Evidence for decreasing quality of semen during past 50 years. *BMJ* 1992;305(September (6854)):609–13.
- [4] Jacobsen R, Moller H, Thoresen SO, Pukkala E, Kjaer SK, Johansen C. Trends in testicular cancer incidence in the Nordic countries, focusing on the recent decrease in Denmark. *Int J Androl* 2006;29(February (1)):199–204.
- [5] Richiardi L, Bellocchio R, Adami HO, Torrang A, Barlow L, Hakulinen T, et al. Testicular cancer incidence in eight northern European countries: secular and recent trends. *Cancer Epidemiol Biomarkers Prev* 2004;13(December (12)):2157–66.
- [6] Walsh TJ, Croughan MS, Schembri M, Chan JM, Turek PJ. Increased risk of testicular germ cell cancer among infertile men. *Arch Intern Med* 2009;169(February (4)):351–6.
- [7] Fraga CG, Motchnik PA, Wyrobek AJ, Rempel DM, Ames BN. Smoking and low antioxidant levels increase oxidative damage to sperm DNA. *Mutat Res* 1996;351(April (2)):199–203.
- [8] Ji BT, Shu XO, Linet MS, Zheng W, Wacholder S, Gao YT, et al. Paternal cigarette smoking and the risk of childhood cancer among offspring of nonsmoking mothers. *J Natl Cancer Inst* 1997;89(February (3)):238–44.
- [9] Hamer G, Roepers-Gajadien HL, van Duyn-Goedhart A, Gademan IS, Kal HB, van Buul PP, et al. DNA double-strand breaks and gamma-H2AX signaling in the testis. *Biol Reprod* 2003;68(February (2)):628–34.
- [10] Olsen AK, Lindeman B, Wiger R, Duale N, Brunborg G. How do male germ cells handle DNA damage? *Toxicol Appl Pharmacol* 2005;207(September (2 Suppl.)):521–31.
- [11] van Loon AA, Sonneveld E, Hoogerbrugge J, van der Schans GP, Grootegeod JA, Lohman PH, et al. Induction and repair of DNA single-strand breaks and

- DNA base damage at different cellular stages of spermatogenesis of the hamster upon in vitro exposure to ionizing radiation. *Mutat Res* 1993;294(August (2)):139–48.
- [12] Xu G, Spivak G, Mitchell DL, Mori T, McCarrey JR, McMahan CA, et al. Nucleotide excision repair activity varies among murine spermatogenic cell types. *Biol Reprod* 2005;73(July (1)):123–30.
- [13] Jansen J, Olsen AK, Wiger R, Naegeli H, de BP, van Der HF, et al. Nucleotide excision repair in rat male germ cells: low level of repair in intact cells contrasts with high dual incision activity in vitro. *Nucleic Acids Res* 2001;29(April (8)):1791–800.
- [14] Olsen AK, Bjortuft H, Wiger R, Holme J, Seeberg E, Bjoras M, et al. Highly efficient base excision repair (BER) in human and rat male germ cells. *Nucleic Acids Res* 2001;29(April (8)):1781–90.
- [15] Olsen AK, Andreassen A, Singh R, Wiger R, Duale N, Farmer PB, et al. Environmental exposure of the mouse germ line: DNA adducts in spermatozoa and formation of de novo mutations during spermatogenesis. *PLoS One* 2010;5(June (6)):e11349.
- [16] Sipinen V, Laubenthal J, Baumgartner A, Cemeli E, Linschooten JO, Godschalk RW, et al. In vitro evaluation of baseline and induced DNA damage in human sperm exposed to benzo[a]pyrene or its metabolite benzo[a]pyrene-7,8-diol-9,10-epoxide, using the comet assay. *Mutagenesis* 2010;25(July (4)):417–25.
- [17] Verhofstad N, van Oostrom CT, van BJ, Van Schooten FJ, van SH, Godschalk RW. DNA adduct kinetics in reproductive tissues of DNA repair proficient and deficient male mice after oral exposure to benzo(a)pyrene. *Environ Mol Mutagen* 2010;51(March (2)):123–9.
- [18] Bjorge C, Brunborg G, Wiger R, Holme JA, Scholz T, Dybing E, et al. A comparative study of chemically induced DNA damage in isolated human and rat testicular cells. *Reprod Toxicol* 1996;10(November (6)):509–19.
- [19] Sega GA, Generoso EE. Measurement of DNA breakage in specific germ-cell stages of male mice exposed to acrylamide, using an alkaline-elution procedure. *Mutat Res* 1990;242(September (1)):79–87.
- [20] Shelby MD, Cain KT, Hughes LA, Braden PW, Generoso WM. Dominant lethal effects of acrylamide in male mice. *Mutat Res* 1986;173(January (1)):35–40.
- [21] Marchetti F, Lowe X, Bishop J, Wyrobek AJ. Induction of chromosomal aberrations in mouse zygotes by acrylamide treatment of male germ cells and their correlation with dominant lethality and heritable translocations. *Environ Mol Mutagen* 1997;30(4):410–7.
- [22] Mottram DS, Wedzicha BL, Dodson AT. Acrylamide is formed in the Maillard reaction. *Nature* 2002;419(October (6906)):448–9.
- [23] Rosen J, Hellenas KE. Analysis of acrylamide in cooked foods by liquid chromatography tandem mass spectrometry. *Analyst* 2002;127(July (7)):880–2.
- [24] Stadler RH, Scholz G. Acrylamide: an update on current knowledge in analysis, levels in food, mechanisms of formation, and potential strategies of control. *Nutr Rev* 2004;62(December (12)):449–67.
- [25] Calleman CJ, Bergmark E, Costa LG. Acrylamide is metabolized to glycidamide in the rat: evidence from hemoglobin adduct formation. *Chem Res Toxicol* 1990;3(September (5)):406–12.
- [26] Ghanayem BI, McDaniel LP, Churchwell MI, Twaddle NC, Snyder R, Fennell TR, et al. Role of CYP2E1 in the epoxidation of acrylamide to glycidamide and formation of DNA and hemoglobin adducts. *Toxicol Sci* 2005;88(December (2)):311–8.
- [27] Settels E, Bernauer U, Palavinskas R, Klaffke HS, Gundert-Remy U, Appel KE. Human CYP2E1 mediates the formation of glycidamide from acrylamide. *Arch Toxicol* 2008;82(October (10)):717–27.
- [28] Sumner SC, Fennell TR, Moore TA, Chanas B, Gonzalez F, Ghanayem BI. Role of cytochrome P450 2E1 in the metabolism of acrylamide and acrylonitrile in mice. *Chem Res Toxicol* 1999;12(November (11)):1110–6.
- [29] Koyama N, Yasui M, Oda Y, Suzuki S, Satoh T, Suzuki T, et al. Genotoxicity of acrylamide in vitro: acrylamide is not metabolically activated in standard in vitro systems. *Environ Mol Mutagen* 2010;(March).
- [30] Rice JM. The carcinogenicity of acrylamide. *Mutat Res* 2005;580(February (1–2)):3–20.
- [31] Sega GA. Unscheduled DNA synthesis (DNA repair) in the germ cells of male mice—its role in the study of mammalian mutagenesis. *Genetics* 1979;92(May (1 Pt 1 Suppl.)):s49–58.
- [32] Sega GA, Alcota RP, Tancongco CP, Brimer PA. Acrylamide binding to the DNA and protamine of spermiogenic stages in the mouse and its relationship to genetic damage. *Mutat Res* 1989;216(August (4)):221–30.
- [33] Gamboa da CG, Churchwell MI, Hamilton LP, Von Tungeln LS, Beland FA, Marques MM, et al. DNA adduct formation from acrylamide via conversion to glycidamide in adult and neonatal mice. *Chem Res Toxicol* 2003;16(October (10)):1328–37.
- [34] Maniere I, Godard T, Doerge DR, Churchwell MI, Guffroy M, Laurentie M, et al. DNA damage and DNA adduct formation in rat tissues following oral administration of acrylamide. *Mutat Res* 2005;580(February (1–2)):119–29.
- [35] Segerback D, Calleman CJ, Schroeder JL, Costa LG, Faustman EM. Formation of N-7-(2-carbamoyl-2-hydroxyethyl)guanine in DNA of the mouse and the rat following intraperitoneal administration of [¹⁴C]acrylamide. *Carcinogenesis* 1995;16(May (5)):1161–5.
- [36] Rodriguez-Zas SL, Schellander K, Lewin HA. Biological interpretations of transcriptomic profiles in mammalian oocytes and embryos. *Reproduction* 2008;135(February (2)):129–39.
- [37] Tadros W, Lipshitz HD. The maternal-to-zygotic transition: a play in two acts. *Development* 2009;136(September (18)):3033–42.
- [38] Stanton JA, Macgregor AB, Green DP. Gene expression in the mouse preimplantation embryo. *Reproduction* 2003;125(April (4)):457–68.
- [39] Harrouk W, Codrington A, Vinson R, Robaire B, Hales BF. Paternal exposure to cyclophosphamide induces DNA damage and alters the expression of DNA repair genes in the rat preimplantation embryo. *Mutat Res* 2000;461(November (3)):229–41.
- [40] Harrouk W, Robaire B, Hales BF. Paternal exposure to cyclophosphamide alters cell-cell contacts and activation of embryonic transcription in the preimplantation rat embryo. *Biol Reprod* 2000;63(July (1)):74–81.
- [41] Bergkvist A, Rusanakova V, Sindelka R, Garda JM, Sjogreen B, Lindh D, et al. Gene expression profiling—clusters of possibilities. *Methods* 2010;50(April (4)):323–35.
- [42] Sindelka R, Ferjentsik Z, Jonak J. Developmental expression profiles of *Xenopus laevis* reference genes. *Dev Dyn* 2006;235(March (3)):754–8.
- [43] Bowman P, McLaren A. Cleavage rate of mouse embryos in vivo and in vitro. *J Embryol Exp Morphol* 1970;24(August (1)):203–7.
- [44] Harlow GM, Quinn P. Development of preimplantation mouse embryos in vivo and in vitro. *Aust J Biol Sci* 1982;35(2):187–93.
- [45] Bischoff M, Parfitt DE, Zernicka-Goetz M. Formation of the embryonic–abembryonic axis of the mouse blastocyst: relationships between orientation of early cleavage divisions and pattern of symmetric/asymmetric divisions. *Development* 2008;135(March (5)):953–62.
- [46] Fujimori T, Kurotaki Y, Komatsu K, Nabeshima Y. Morphological organization of the mouse preimplantation embryo. *Reprod Sci* 2009;16(February (2)):171–7.
- [47] Kurotaki Y, Hatta K, Nakao K, Nabeshima Y, Fujimori T. Blastocyst axis is specified independently of early cell lineage but aligns with the ZP shape. *Science* 2007;316(May (5825)):719–23.
- [48] Shannon P, Markiel A, Ozier O, Baliga NS, Wang JT, Ramage D, et al. Cytoscape: a software environment for integrated models of biomolecular interaction networks. *Genome Res* 2003;13(November (11)):2498–504.
- [49] Marchetti F, Wyrobek AJ. Mechanisms and consequences of paternally-transmitted chromosomal abnormalities. *Birth Defects Res C: Embryo Today* 2005;75(June (2)):112–29.
- [50] Shelby MD. Selecting chemicals and assays for assessing mammalian germ cell mutagenicity. *Mutat Res* 1996;352(June (1–2)):159–67.
- [51] Pacchierotti F, Tiveron C, D'Archivio M, Bassani B, Cordelli E, Leter G, et al. Acrylamide-induced chromosomal damage in male mouse germ cells detected by cytogenetic analysis of one-cell zygotes. *Mutat Res* 1994;309(September (2)):273–84.
- [52] Yamauchi Y, Shaman JA, Ward WS. Non-genetic contributions of the sperm nucleus to embryonic development. *Asian J Androl* 2010;(October).
- [53] Grinfeld S, Jaquet P. An unusual radiation-induced G2 arrest in the zygote of the BALB/c mouse strain. *Int J Radiat Biol Relat Stud Phys Chem Med* 1987;51(February (2)):353–63.
- [54] Jurisicova A, Latham KE, Casper RF, Casper RF, Varmuza SL. Expression and regulation of genes associated with cell death during murine preimplantation embryo development. *Mol Reprod Dev* 1998;51(November (3)):243–53.
- [55] Schmidt-Kastner PK, Jardine K, Cormier M, McBurney MW. Absence of p53-dependent cell cycle regulation in pluripotent mouse cell lines. *Oncogene* 1998;16(June (23)):3003–11.
- [56] Mukherjee AB. Cell cycle analysis and X-chromosome inactivation in the developing mouse. *Proc Natl Acad Sci USA* 1976;73(May (5)):1608–11.
- [57] Kamjoo M, Brison DR, Kimber SJ. Apoptosis in the preimplantation mouse embryo: effect of strain difference and in vitro culture. *Mol Reprod Dev* 2002;61(January (1)):67–77.
- [58] Meseguer M, Martinez-Conejero JA, O'Connor JE, Pellicer A, Remohi J, Garrido N. The significance of sperm DNA oxidation in embryo development and reproductive outcome in an oocyte donation program: a new model to study a male infertility prognostic factor. *Fertil Steril* 2008;89(May (5)):1191–9.
- [59] Marchetti F, Bishop J, Lowe X, Wyrobek AJ. Chromosomal mosaicism in mouse two-cell embryos after paternal exposure to acrylamide. *Toxicol Sci* 2009;107(January (1)):194–205.
- [60] Barton TS, Robaire B, Hales BF. Epigenetic programming in the preimplantation rat embryo is disrupted by chronic paternal cyclophosphamide exposure. *Proc Natl Acad Sci USA* 2005;102(May (22)):7865–70.
- [61] Barton TS, Robaire B, Hales BF. DNA damage recognition in the rat zygote following chronic paternal cyclophosphamide exposure. *Toxicol Sci* 2007;100(December (2)):495–503.
- [62] Adler ID, Baumgartner A, Gonda H, Friedman MA, Skerhut M. 1-Aminobenzotriazole inhibits acrylamide-induced dominant lethal effects in spermatids of male mice. *Mutagenesis* 2000;15(March (2)):133–6.
- [63] Generoso WM, Sega GA, Lockhart AM, Hughes LA, Cain KT, Cacheiro NL, et al. Dominant lethal mutations, heritable translocations, and unscheduled DNA synthesis induced in male mouse germ cells by glycidamide, a metabolite of acrylamide. *Mutat Res* 1996;371(December (3–4)):175–83.
- [64] Adler ID, Reitmeir P, Schmoller R, Schriever-Schwemmer G. Dose response for heritable translocations induced by acrylamide in spermatids of mice. *Mutat Res* 1994;309(September (2)):285–91.
- [65] de la Chapelle A. Genetic predisposition to colorectal cancer. *Nat Rev Cancer* 2004;4(October (10)):769–80.
- [66] Cloos PA, Christensen J, Agger K, Maiolica A, Rappsilber J, Antal T, et al. The putative oncogene GASC1 demethylates tri- and dimethylated lysine 9 on histone H3. *Nature* 2006;442(July (7100)):307–11.

- [67] Ishimura A, Terashima M, Kimura H, Akagi K, Suzuki Y, Sugano S, et al. Jmjd2c histone demethylase enhances the expression of Mdm2 oncogene. *Biochem Biophys Res Commun* 2009;389(November (2)):366–71.
- [68] Shimura T, Toyoshima M, Taga M, Shiraishi K, Uematsu N, Inoue M, et al. The novel surveillance mechanism of the Trp53-dependent s-phase checkpoint ensures chromosome damage repair and preimplantation-stage development of mouse embryos fertilized with x-irradiated sperm. *Radiat Res* 2002;158(December (6)):735–42.
- [69] Shimura T, Inoue M, Taga M, Shiraishi K, Uematsu N, Takei N, et al. p53-dependent S-phase damage checkpoint and pronuclear cross talk in mouse zygotes with X-irradiated sperm. *Mol Cell Biol* 2002;22(April (7)):2220–8.
- [70] Toyoshima M, Shimura T, Adiga SK, Taga M, Shiraishi K, Inoue M, et al. Transcription-independent suppression of DNA synthesis by p53 in sperm-irradiated mouse zygotes. *Oncogene* 2005;24(May (20)):3229–35.